INVERSION OF PARTICLE SIZE DISTRIBUTION BY SPECTRAL EXTINCTION TECHNIQUE USING THE ATTRACTIVE AND REPULSIVE PARTICLE SWARM OPTIMIZATION ALGORITHM

by

Hong QI, Zhen-Zong HE, Shuai GONG, and Li-Ming RUAN *

School of Energy Science and Engineering, Harbin Institute of Technology, Harbin, China

Original scientific paper
DOI: 10.2298/TSCI140319103Q

The particle size distribution plays an important role in environmental pollution detection and human health protection, such as fog, haze, and soot. In this study, the attractive and repulsive particle swarm optimization algorithm and the basic particle swarm optimization were applied to retrieve the particle size distribution. The spectral extinction technique coupled with the anomalous diffraction approximation and the Lambert-Beer law were employed to investigate the retrieval of the particle size distribution. Three commonly used monomodal particle size distribution, i. e. the Rosin-Rammer distribution, the normal distribution, the logarithmic normal distribution were studied in the dependent model. Then, an optimal wavelengths selection algorithm was proposed. To study the accuracy and robustness of the inverse results, some characteristic parameters were employed. The research revealed that the attractive and repulsive particle swarm optimization showed more accurate and faster convergence rate than the basic, particle swarm optimization even with random measurement error. Moreover, the investigation also demonstrated that the inverse results of four incident laser wavelengths showed more accurate and robust than those of two wavelengths. The research also found that if increasing the interval of the selected incident laser wavelengths, inverse results would show more accurate, even in the presence of random error.

Key words: *inverse problem, the attractive and repulsive particle swarm optimization, particle size distribution, spectral extinction*

Introduction

Particle size often plays an important role in the production quality control of industry, environmental pollution detection, and human health protection, *etc*., so it is very important to on-line monitor the granularity to provide real-time measurements of both the size distribution and the concentration of the particle system in the industrial applications and other related fields [1, 2]. For instance, it is necessary to know the particle size distribution (PSD) of micrometric or submicrometric particles in measurement and control of fuel sprays, powder suspensions, atmospheric aerosols, and other particulate pollutions. Unfortunately, the PSD usually cannot be measured directly, and it can only be retrieved with the help of some experimental data and corresponding inverse theories. The light scattering particle sizing technique, which is a fast,

* Corresponding author; e-mail: ruanlm@hit.edu.cn

non-intrusive and convenient method, coupled with some intelligent optimization algorithms has been applied to retrieve the PSD in recent years [1, 3]. In order to infer the PSD using the light scattering techniques, many attractive methods have emerged during the past two decades, *e. g*., the spectral extinction measurement, forward scattering measurement, combined scattering and extinction measurement, angular scattering measurement, backscattering measurement, and the polarization measurement [4]. Among all these methods, the spectral extinction measurement is regard as one of the most potential techniques for only requiring a simple optical layout and a commercial spectrophotometer. The calculation of the extinction efficiency is very important and usually calculated by the Mie theory [3, 5]. However, the calculation of extinction efficiency based on Mie theory for spherical particles is complicated and time-consuming. Additionally, the Mie theory can only be applied to the homogeneous spherical particle, while most particle systems are non-spherical particles. To overcome these difficulties, many rigorous numerical methods have been developed to calculate the absorption and scattering properties of the non-spherical particles. The anomalous diffraction approximation (ADA) which was introduced by Van de Hulst [6] firstly, is regard as a kind of most potential algorithm to calculate the extinction efficiency of spherical and spheroidal particles for its simple but accurate approximation formula [7]. Both numerical simulation and experimental results demonstrate that the ADA can be successfully applied to retrieve the PSD for spherical and spheroidal particles with high accuracy and stability, even in the presence of random error [8, 9].

The development of stable and robust methods to determine the PSD accurately has long been considered as an unsolved problem, and needs further research. Generally speaking, the methods for retrieving PSD can be broadly classified into three different categories, *e. g*. the analytic inversion model, the dependent model and the independent model [3, 8]. The analytic inversion model is that the integral equation is retrieved analytically by using an approximate scattering kernel. The dependent model is the widely used method, and its basic idea is that the PSD is retrieved using a certain optimization algorithm with an assuming priori PSD information. The independent model is that the PSD is retrieved by measuring the extinction efficiency of multi-wavelengths and solving the Fredholm integral equation of the first kind without priori information about the PSD [8, 10]. Theoretically speaking, the first kind Fredholm integral equations are typically ill-posed and hard to be solved directly. Fortunately, most particle systems can often be approximately regarded as obeying certain kind of PSD, so the dependent model is extensively studied and applied in many fields [3, 8]. Recently, a very considerable amount of random search intelligent algorithms have been proposed to solve the inverse PSD problem under dependent model, such as the multi-phase particle swarm optimization, the genetic algorithms, the general regression neural networks, and the ant colony optimization, *etc*. [1, 10-12]. Among all these intelligent algorithms, the particle swarm optimization (PSO), algorithm first introduced in 1995 by Kennedy and Eberhart [13], is characterized to be simple in concept, easy to implement, and computationally efficient. Unlike other heuristic techniques, the PSO has a flexible and well-balanced mechanism to enhance the global and local exploration abilities, which has been studied extensively to solve inverse radiation problems in recent years [14, 15]. However, the basic PSO technique has the disadvantages of time-consuming and premature convergence, so there is a substantial need to look for improvements. In present paper, an improved attractive and repulsive particle swarm optimization (ARPSO) algorithm [16], which is characterized by using a diversity measurement to alternate between phases of attraction and repulsion in trying to overcome the premature convergence, was applied to solve the inverse problem for determining the PSD. Three commonly used monomodal PSD, *i. e*., the Rosin-Rammer (R-R) function, the normal (N-N) function, and the logarithmic normal (L-N)

function, were retrieved to investigate the performance of ARPSO in the dependent model first. Then, an optimal wavelength selection algorithm was recommended.

Theories and methods

The principle of the light extinction method

According to the Lambert-Beer law and the single scattering approximation, when a collimated light beam of intensity I_0 irradiates on a suspension particle system, the transmitted light is scattered and absorbed by the particles, which causes the attenuation of the light. If the optical thickness of the particle system is thin and the independent scattering dominates, the transmitted light intensity I with the incident wavelength λ can be calculated [17]:

$$\ln\frac{I(\lambda)}{I_0(\lambda)} = -\frac{3}{2}LN_{\mathrm{D}}\int_{D_{\min}}^{D_{\max}}\frac{Q_{\mathrm{ext}}(\lambda, m, D)}{D}f(D)\mathrm{d}D \tag{1}$$

where $Q_{\mathrm{ext}}(\lambda, m, D)$ is the extinction efficiency of particles which is a complex function of the particle diameter D, λ – the wavelength of incident light, and m – the complex refractive index. The $I_0(\lambda)$ is the incident light intensity at wavelength λ. The ratio value $I(\lambda)/I_0(\lambda)$ is obtained by actual measurements. The N_{D} [m^{-3}] is the total number of particles per unit volume. The $D_{\max}$ and $D_{\min}$ are the upper and lower integration limits, respectively. The $f(D)$ is the volume frequency distribution of particle system with a diameter between D and $D + \mathrm{d}D$, which needs to be determined. The L is the geometrical thickness of the particle system [18]. The extinction efficiency for a spherical particle can be deduced from the ADA and described as [19]:

$$Q_{\mathrm{ext}}(\lambda, m, D) = 4\,\mathrm{Re}\left[\frac{1}{2} - i\frac{\exp(-i\rho)}{\rho} + \frac{1-\exp(-i\rho)}{\rho^2}\right] \tag{2}$$

where $\rho = \pi D(m-1)/\lambda$, $i = (-1)^{1/2}$.

The principle of the ARPSO

For the sake of brevity, the details of the basic PSO used in this study are available in [14], and not repeated here. In the basic PSO, the fast information flow between particles seems to be the reason for clustering of particles. Diversity declines rapidly, leaving the PSO with great difficulties of escaping local optima. Consequently, the clustering leads to low diversity with fitness stagnation as an overall result. Compared with the basic PSO, the ARPSO can overcome the problem of premature convergence which is a major problem with evolutionary algorithms in multi-modal optimization and results in great performance loss and sub-optimal solutions [16]. In ARPSO, the attraction phase is defined as the basic PSO. The particles would then attract each other, since in general they attract each other in the basic PSO because of the information flow of good solution between particles. The second phase repulsion is also defined by *inverting* the velocity-update formula of the particles. The velocity-update formula can be described [16]:

$$\vec{\mathrm{V}}_i(t+1) = \omega\vec{\mathrm{V}}_i(t) + \mathrm{dir}\{C_1[\vec{\mathrm{P}}_i(t) - \vec{\mathrm{X}}_i(t)] + C_2[\vec{\mathrm{P}}_g(t) - \vec{\mathrm{X}}_i(t)]\} \tag{3}$$

$$\vec{\mathrm{X}}_i(t+1) = \vec{\mathrm{X}}_i(t) + \vec{\mathrm{V}}_i(t+1) \tag{4}$$

where parameter ω is the inertia weight and controls the magnitude of the old velocity $\vec{\mathrm{V}}_i(t)$ in the calculation of the new velocity $\vec{\mathrm{V}}_i(t+1)$, C_1 and C_2 – are two positive constants called acceleration coefficients, $\vec{\mathrm{P}}_i(t)$, and $\vec{\mathrm{P}}_{\mathrm{g}}(t)$ – are the best position of the i^{th} particle and the global best

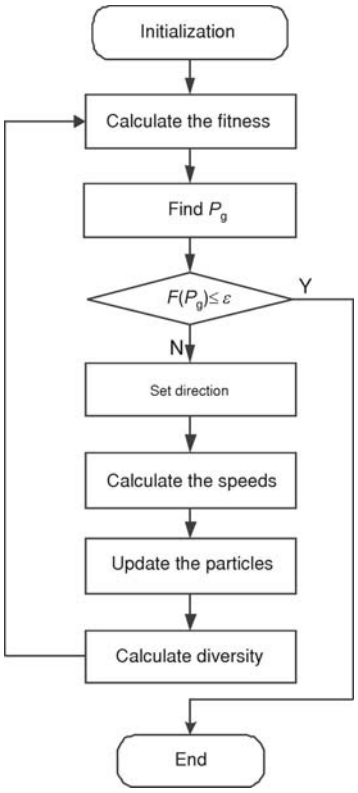

Figure 1. The flowchart of the ARPSO

position of all the particles, respectively, $\vec{X}_i(t)$ and $X_i(t+1)$ – are the old and new position of the i^{th} particle, dir – is the sign-variable, either to 1 or –1 depending on the diversity, which decides directly whether the particles attract or repel each other. The diversity of the swarm (in the pseudo-code stored in the variable *diversity*) is set according to the diversity-measure [16]:

$$\text{diversity}(S) = \frac{1}{|S||L|}\sum_{i=1}^{|S|}\sqrt{\sum_{j=1}^{N}(x_{ij} - \overline{x_j})^2} \tag{5}$$

where S is the swarm, $|S|$ – the swarm size, $|L|$ – the length of the longest diagonal in the search space, N – the dimensionality of the problem, x_{ij} – the j^{th} value of the i^{th} particle, $\overline{x_j}$ – the j^{th} value of the average point $\bar{x}$. Note that this diversity measurement is dependent of swarm size, the dimensionality of the problem as well as the search range in each dimension. When the driversity drops below the lower bound d_{low}, the ARPSO switches to the repulsion phase and the *dir* in eq. (3) is set as –1. When the diversity of d_{high} is reached, the ARPSO changes back to the attractive phase and the *dir* is set as 1 [16]. The flowchart of the ARPSO is shown in fig. 1.

Results and discussions

In the dependent model, three kinds of widely used monomodal functions, *e. g.* the R-R function, the N-N function, and the L-N function, were studied. The mathematical representations of their monomodal volume frequency distributions are [1]:

$$f_{R-R}(D) = \frac{k'}{\overline{D}}\left(\frac{D}{\overline{D}}\right)^{k'-1}\exp\left[-\left(\frac{D}{\overline{D}}\right)^{k'}\right] \tag{6}$$

$$f_{\text{N-N}}(D) = \frac{1}{\sqrt{2\pi}\sigma_{\text{N}}}\exp\left[-\frac{(D-\mu_{\text{N}})^2}{2\sigma_N^2}\right] \tag{7}$$

$$f_{\text{L-N}}(D) = \frac{1}{\sqrt{2\pi}D\ln\sigma_{\text{L}}}\exp\left[-\frac{(\ln D - \ln\mu_{\text{L}})^2}{2(\ln\sigma_{\text{L}})^2}\right] \tag{8}$$

where $\overline{D}, k', \mu_{\text{N}}, \sigma_{\text{N}}, \mu_{\text{L}}$, and σ_{L} are the characteristic parameters, and D is the diameter of the particle. The complex refraction index used in this paper refers to [20], and the real part n and the imaginary part k of it are in the range of $n \in [1.18, 1.92]$ and $k \in [0.01, 1.13]$, respectively. The complex refractive index in this article is set as $1.50 + 0.02i$, which is assumed to be constant at different wavelengths for the sake of simplicity.

The wavelengths of the incident light are set as $\lambda = 0.45$, and 0.50 μm in two wavelengths model and $\lambda = 0.45$, 0.50, 0.55, and 0.6 μm in four wavelengths model. The size measurement range of the particles is selected from 0.1 μm to 10 μm, which is the optimal measurement range in the spectral extinction particle size technique. The true values of the PSD which

are studied in the thesis are fixed as $(\overline{D}, k') = (2.0, 1.9)$, $(\mu_N, \sigma_N) = (3.2, 2.0)$, and $(\mu_L, \sigma_L) = 2.0$, 2.0), respectively. The basic PSO and the ARPSO are used to retrieve these spherical PSD in the dependent model, respectively. The retrieval of the spherical PSD is solved by minimizing the objective function, which is the sum of the square residuals between the estimated and measured transmittances:

$$F_{\text{obj}} = \sum_{i=1}^{N_\lambda} \left\{ \frac{\left[\dfrac{I(\lambda)}{I_0(\lambda)}\right]_{\text{est}} - \left[\dfrac{I(\lambda)}{I_0(\lambda)}\right]_{\text{mea}}}{\left[\dfrac{I(\lambda)}{I_0(\lambda)}\right]_{\text{mea}}} \right\}^2 \tag{9}$$

where N_λ is the number of the wavelengths. When the value of F_{obj} is less than the tolerance ε or the maximum iterative number *maxgens* is reached, the calculations end. The system control parameters in these two algorithms are described in tab. 1. Taking into account the fact that the ARPSO and the basic PSO are stochastic optimization methods and all optimizations have certain randomness, both of them are repeated 50 times for each of these PSD. The effect of the random measurement errors is also considered in the calculation. Moreover, for the purpose of investigating the reliability and feasibility of this optimization algorithm, some characteristic parameters used to evaluate the quality of inversion results are studied as follows.

Table 1. The parameters of the ARPSO and the basic PSO for different PSD functions

Parameter value	C_1	C_2	d_{high}	d_{low}	|S|	N	$[d_{low}, d_{high}]$	V_{max}	maxgens	ε
ARPSO	2.0	2.0	0.25	$5.0 \cdot 10^{-6}$	50	2	[0, 10]	10.0	5000	10^{-8}
PSO	2.0	2.0	N/A	N/A	50	2	[0, 10]	10.0	5000	10^{-8}

(1) The relative deviation of PSD δ means the sum of the deviation between the probability distribution estimated from the inverse calculation and the true PSD in every subinterval. For spherical particles, the mathematic expression of δ is [12]:

$$\delta = \frac{\sqrt{\sum_{i=1}^{N'} [f_{\text{est}}(\widetilde{D}_i) - f_{\text{true}}(\widetilde{D}_i)]^2}}{\sqrt{\sum_{i=1}^{N'} [f_{\text{true}}(\widetilde{D}_i)]^2}} \tag{10}$$

where N' represents the number of subintervals that the size ranges of D $[D_{\text{high}}, D_{\text{low}}]$ are divided; $\widetilde{D}_i$ – the midpoint of the i^{th} subinterval $[D_i, D_{i+1}]$. It is obvious that the smaller the value of δ is, the more accurate the estimated results are.

(2) The average computational time for every iteration convergence $\bar{t}$ is expressed in second.

Tables 2-4 list the retrieval results of three commonly used monomodal PSD functions under dependent model using the ARPSO and PSO algorithms, and the corresponding inverse results are depicted in figs. 2-7. From tab. 2 and fig. 2, it can be seen that for the R-R distribution when there is no random measurement error, the value of relative deviation δ retrieved by the ARPSO is far less than that of the PSO. When adding the random measurement error to the spectral extinction date, the value of δ will increase, but it is still easy to find that value of δ retrieved by the ARPSO is less than that by the PSO. That is to say, the accuracy and robustness of the in-

Table 2. The retrieval results of the R-R distribution with ($\overline{D}$,k') = (2.0, 1.9)

Model	Error	ARPSO				PSO			
		$\overline{D}$	k'	δ	$\bar{t}$ [s]	$\overline{D}$	k'	δ	$\bar{t}$ [s]
Two wavelengths model	0%	2.00	1.90	0.000073	3.63	1.96	2.53	0.263745	15.17
	2%	1.94	2.28	0.169962	4.73	1.93	2.86	0.380146	16.41
	5%	1.89	3.30	0.525782	8.16	1.88	3.52	0.590838	19.16
Four wavelengths model	0%	2.00	1.90	0.000061	5.70	1.97	1.94	0.024552	28.71
	2%	1.99	1.91	0.007707	23.68	1.97	1.96	0.029896	30.41
	5%	1.96	1.97	0.037481	24.50	1.97	1.99	0.045179	31.40

* The mean inverse results and relative deviation of the 50 times calculations are shown in the table

Table 3. The retrieval results of the N-N distribution with (μ_N, σ_N) = (3.2, 2.0)

Model	Error	ARPSO				PSO			
		μ_N	σ_N	δ	$\bar{t}$ [s]	μ_N	σ_N	δ	$\bar{t}$ [s]
Two wavelengths model	0%	3.20	2.00	0.000069	3.22	2.93	1.66	0.194042	16.36
	2%	2.75	2.13	0.142325	6.90	2.90	1.46	0.311713	16.48
	5%	2.79	1.25	0.475353	8.22	1.76	1.51	0.623876	17.70
Four wavelengths model	0%	3.20	2.00	0.000025	2.82	3.16	2.10	0.041733	20.35
	2%	3.18	2.01	0.005566	18.80	3.06	1.97	0.047180	22.24
	5%	3.04	1.94	0.058735	19.87	2.90	1.75	0.163021	27.82

* The mean inverse results and relative deviation of the 50 times calculations are shown in the table

Table 4. The retrieval results of the L-N distribution with (μ_L, σ_L) = (2.0, 2.0)

Model	Error	ARPSO				PSO			
		μ_L	σ_L	δ	$\bar{t}$ [s]	μ_L	σ_L	δ	$\bar{t}$ [s]
Two wavelengths model	0%	1.97	1.96	0.026765	5.09	1.96	1.94	0.039545	14.11
	2%	1.95	1.94	0.037661	5.71	1.92	1.85	0.108919	15.20
	5%	2.05	2.08	0.054171	12.25	1.91	1.82	0.132594	18.81
Four wavelengths model	0%	2.00	2.01	0.000005	5.30	2.00	2.00	0.000392	27.36
	2%	2.01	2.02	0.007210	23.35	1.98	1.96	0.023737	29.81
	5%	1.96	1.94	0.037834	23.77	1.96	1.94	0.042433	31.25

* The mean inverse results and relative deviation of the 50 times calculations are shown in the table

verse results retrieved by the ARPSO are higher than those by the PSO, even with random measurement error. Moreover, the convergence time required by the ARPSO is less than that by the PSO, especially without random measurement error. It is also obvious that increasing the value of the random error, the estimated results deteriorate and the convergence time increases. From tab. 2 and fig. 5, it can be seen that when the R-R distribution is estimated under 5% random measurement error in two wavelengths model, the value of δ is large and the deviations between

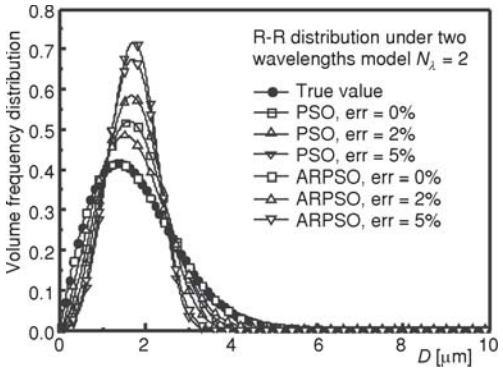

Figure 2. Results for R-R distribution retrived by the ARPSO and the basic PSO under two wavelengths model

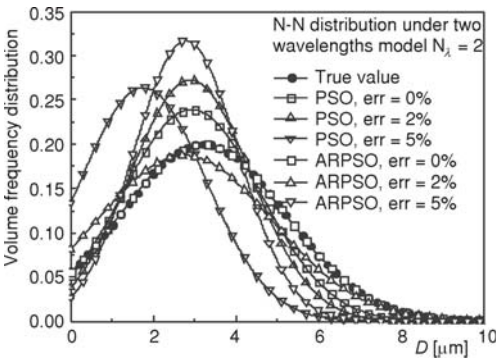

Figure 3. Results for N-N distribution retrived by the ARPSO and the basic PSO under two wavelengths model

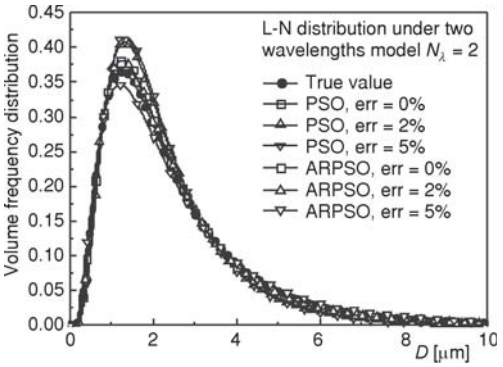

Figure 4. Results for L-N distribution retrived by the ARPSO and the basic PSO under two wavelengths model

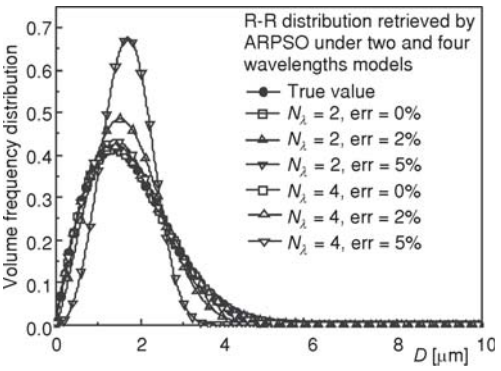

Figure 5. Results for R-R distribution retrived by the ARPSO under two and four wavelengths models

the estimated results and true values, which are depicted in fig. 5, cannot be ignored. Nevertheless, the accuracy and robustness of the inverse results using four wavelengths are still satisfactory. In other words, the results estimated using four wavelengths are better than those using two wavelengths, although the four wavelengths need a little more convergence time. The reason is that two wavelengths offer less transmitted light information which may lead to the multi-valued retrieval results more easily, compared with using four wavelengths. Therefore, although more incident wavelengths will require a little more convergence time, the four wavelengths are recommended to retrieve the PSD of three commonly used monomodal dis-

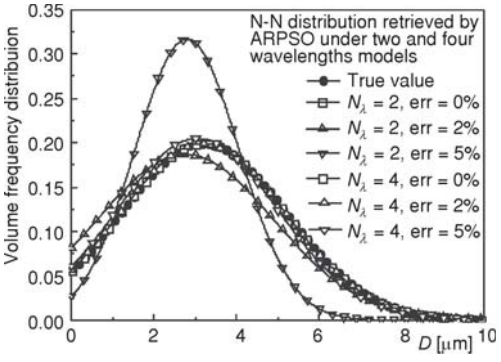

Figure 6. Results for N-N distribution retrieved by the ARPSO under two and four wavelengths models

tribution functions for high inverse accuracy and robustness. The same conclusion can also be drawn in investigating the N-N distribution and the L-N distribution.

Since the spectral extinction data contain some important information about the particle system, it is necessary to study the influence of the spectrum on the retrieval of the PSD. So, for any given PSD, there is an optimum choice of the incident laser wavelengths. Table 5 lists the retrieval results of N-N distribution by the ARPSO with different choice incident laser wavelengths, which are selected according to the arithmetic sequence. The inverse results with 2% and 5% random errors are depicted in

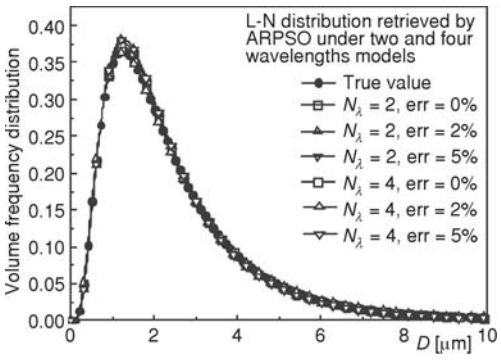

Figure 7. Results for L-N distribution retrieved by the ARPSO under two and four wavelengths models

Table 5. The retrieval results of the N-N distribution by ARPSO with (μ_N, σ_N) = (3.2, 2.0)

	D_λ/μm	($\lambda_1, \lambda_2, \lambda_3, \lambda_4$)/μm	Inversion results		Relative deviation δ	
			Error = 2%	Error = 5%	Error = 2%	Error = 5%
No. 1	0.017	(0.40, 0.417, 0.434, 0.45)	(2.5654, 1.8901)	(2.0546, 1.4477)	0.230657	0.568339
No. 2	0.033	(0.40, 0.433, 0.466, 0.50)	(3.0228, 1.8091)	(2.3815, 1.5428)	0.111599	0.415098
No. 3	0.05	(0.40, 0.45, 0.50, 0.55)	(3.1724, 1.9955)	(2.7440, 1.9674)	0.009767	0.156794
No. 4	0.1	(0.40, 0.50, 0.60, 0.70)	(3.1897, 2.0106)	(3.0949, 2.0187)	0.005286	0.035385
No. 5	0.2	(0.40, 0.60, 0.80, 1.00)	(3.1952, 1.9925)	(3.1434, 1.9321)	0.003611	0.036411
No. 6	0.3	(0.40, 0.70, 1.00, 1.30)	(3.1988, 1.9987)	(3.1976, 1.9691)	0.000692	0.012962

* The mean inverse results and relative deviation of the 50 times calculations are shown in the table

fig. 8 and fig. 9, respectively. From fig. 8, it is easy to see that when the number of the incident wavelengths is fixed and the value of the interval between two incident laser wavelengths $\Delta\lambda$ is equal to 0.05 μm, there is a reasonable agreement between the estimated results and true values of N-N distribution. While $\Delta\lambda$ is larger than 0.05 μm, the accuracy of the inverse results will not be obviously improved with increasing $\Delta\lambda$. From fig. 9, the similar conclusions can be drawn if $\Delta\lambda$ is larger than 0.1 μm. In other words, the larger the value of the common difference is, the more accurate and robust the inverse results will be. The reasons may be that for certain suspension particle system, if the incident laser wavelengths are close to each other, the spectral extinction data will contain less effective information which may weaken the benefits of the multi-spectrum measurement and

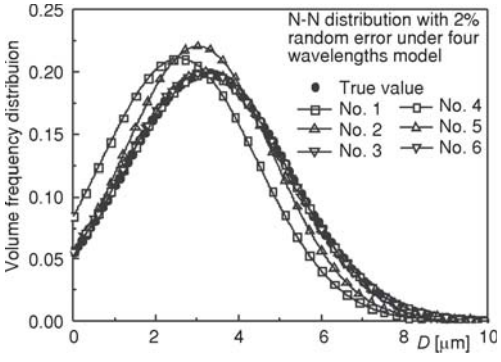

Figure 8. Results for N-N distribution retrieved by the ARPSO with 2% random error

lead to worse inverse results. Therefore, when the spectral extinction technique is applied to investigate the PSD, the interval of incident laser wavelengths should be selected large enough to avoid non-effective measured information and improve the accuracy of the inverse results.

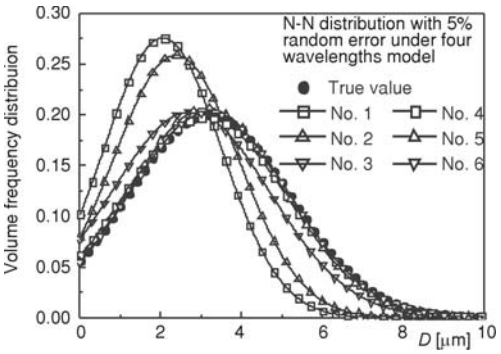

Figure 9. Results for N-N distribution retrieved by the ARPSO with 5% random error

Conclusions

Based on the ADA and the Lambert-Beer theory, the basic PSO and the diversity-guided ARPSO algorithms are employed to determine the PSD under dependent model. By introducing the attractive and repulsive phase depending on the diversity to overcome the premature convergence, the ARPSO algorithm can estimate the retrieval PSD more accurately than basic PSO algorithm. Moreover, the investigation reveals that the more incident wavelengths are employed, the more accurate the inverse results will be, although more convergent time is required. The study also demonstrates that when the number of the incident wavelengths is fixed, larger value of the interval between the selected incident wavelengths can bring in higher accuracy of the inverse results. In conclusion, the optimization algorithm ARPSO is proved to be fast and robust, which has the potential to be implemented in the field of various retrieval PSD problems. In addition, more incident wavelengths and larger value of the interval between the selected wavelengths can be chosen as far as possible for higher inverse accuracy.

Acknowledgment

The supports of this work by the Foundation for Innovative Research Groups of the National Natural Science Foundation of China (No. 51121004), the Major National Scientific Instruments and Equipment Development Special Foundation of China (No. 51327803), and the Specialized Research Fund for the Doctoral Program of Higher Education (No. 20122302110046) are gratefully acknowledged. A very special acknowledgment is made to the editors and referees who make important comments to improve this paper.

Nomenclature

D – diameter of particles, [μm]
F_{obj} – objective function value, [–]
$f(D)$ – the volume frequency distribution, [–]
I – radiative intensity, [$\text{Wm}^{-2}\text{sr}^{-1}$]
L – the geometrical thickness, [m]
m – the complex refractive index, [–]
N – dimensionality of the problem, [–]
N_{D} – the total number of particles, [–]
$\vec{\text{V}}_i$ – velocity, [–]
P_{ij} – the j^{th} value of the i^{th} particle, [–]
$\vec{\text{P}}_i$ – the best position of the i^{th} particle, [–]
P_g – the global best position, [–]
Q_{ext} – the extinction efficiency, [–]
$|S|$ – swarmsize, [–]
$\vec{\text{X}}_i$ – location, [–]

Greek symbols

δ – relative deviation of PSD, [–]
ε – the tolerance, [–]
λ – the wavelength of laser, [μm]
ω – inertia weight, [–]

Subscripts

est – estimated value
ext – extinction efficiency
high – high limit of the search space
low – low limit of the search space
max – the maximum value
mea – the measurement value
min – the minimum value
true – the true value
obj – objective function

References

[1] Qi, H., *et al*., Application of Multi-Phase Particle Swarm Optimization Technique to Retrieve the Particle Size Distribution, *Chinese Optics Letters, 6* (2008), 5, pp. 346-349
[2] Qin, S., Cai, X. S., Indirect Measurement of the Intensity of Incident Light by the Light Transmission Fluctuation Method, *Optics Letters, 36* (2011), 20, pp. 4068-4070
[3] Tang, H., *et al.*, Calculation Method for Particle Mean Diameter and Particle Size Distribution Function under Dependent Model Algorithm, *Chinese Optics Letters, 5* (2007), 1, pp. 31-33
[4] Arias, M. L., Frontini, G. L., Particle Size Distribution Retrieval from Elastic Light Scattering Measurements by a Modified Regularization Method, *Particle & Particle Systems Characterization, 23* (2006), 5, pp. 374-380
[5] Tang, H., Lin, J. Z., Retrieval of Spheroid Particle Size Distribution from Spectral Extinction Data in the Independent Mode Using PCA Approach, *Journal of Quantitative Spectroscopy and Radiative Transfer, 115* (2012), Jan., pp. 78-92
[6] Hulst, H. C., *Light Scattering: by Small Particles*, Courier Dover Publications, New York, N. Y., USA, 1957
[7] Zhao, J. Q., Hu, Y. Q., Bridging Technique for Calculating the Extinction Efficiency of Arbitrary Shaped Particles, *Applied Optics, 42* (2003), 24, pp. 4937-4945
[8] Sun, X. G., *et al*., Anomalous Diffraction Approximation Method for Retrieval of Spherical and Spheroidal Particle Size Distributions in Total Light Scattering, *Journal of Quantitative Spectroscopy and Radiative Transfer, 109* (2008), 1, pp. 89-106
[9] Tang, H., Optimal Wavelength Selection Algorithm of Non-Spherical Particle Size Distribution Based on the Light Extinction Data, *Thermal Science, 16* (2012), 5, pp. 1353-1357
[10] Ye, M., *et al*., Inversion of Particle-Size Distribution from Angular Light-Scattering Data with Genetic Algorithms, *Applied Optics, 38* (1999), 12, pp. 2677-2685
[11] Gugliotta, L. M., *et al*., A Neural Network Model for Estimating the Particle Size Distribution of Dilute Latex from Multiangle Dynamic Light Scattering Measurements, *Particle & Particle Systems Characterization, 26* (2009), 12, pp. 41-52
[12] Qi, H., *et al.*, Retrieval of Spherical Particle Size Distribution Using Ant Colony Optimization Algorithm, *Chinese Optics Letters, 11* (2013), 11, pp. 112901
[13] Kennedy, J., Eberhart, R., Particle Swarm Optimization, *Proceedings,* IEEE International Conference on Neural Networks, IEEE Press, Perth, Australia, 1995, Vol. 4, pp. 1942-1948
[14] Qi, H., *et al.*, Inverse Radiation Analysis of a One-Dimensional Participating Slab by Stochastic Particle Swarm Optimizer Algorithm, *International Journal of Thermal Sciences, 46* (2007), 7, pp. 649-661
[15] Lee, K. H., *et al*., Inverse Radiation Analysis Using Repulsive Particle Swarm Optimization Algorithm, *International Journal of Heat and Mass Transfer, 51* (2008), 11-12, pp. 2772-2783
[16] Riget, J., Vesterstrøm, J. S., A Diversity-Guided Particle Swarm Optimizer-the ARPSO, Report No. 2002-02, University of Aarhus, Aarhus, Denmark, 2002
[17] Tang, H., Retrieval of Spherical Particle Size Distribution with an Improved Tikhonov Iteration Method, *Thermal Science, 16* (2012), 5, pp. 1400-1404
[18] He, Z. Z., *et al*., Inverse Estimation of the Spheroidal Particle Size Distribution Using Ant Colony Optimization Algorithms in Multispectral Extinction Technique, *Optics Communications, 328* (2014), Oct., pp. 8-22
[19] Zhao, J. Q., Li, J. N., Analytical Transform Techniques to Retrieve Non-Spherical Particle Size Distribution, *Journal of Quantitative Spectroscopy and Radiative Transfer, 129* (2013), Nov., pp. 287-297
[20] Ruan, L. M., *et al*., A Transmission Method for the Determination of the Radiation Properties of Small Ash Particles, *Journal of Harbin Institute of Technology, 2* (1994), 2, pp. 10-14

Paper submitted: March 19, 2014
Paper revised: June 8, 2014
Paper accepted: July 30, 2104